

Synthesis, Photophysics, and Electroluminescence of Copolyfluorenes Containing DCM Derivatives

Bar-Yuan Hsieh and Yun Chen*

Department of Chemical Engineering, National Cheng Kung University, Tainan, Taiwan, Republic of China

Received June 8, 2007; Revised Manuscript Received August 28, 2007

ABSTRACT: New copolyfluorenes (**PFD0.5–50**) of 9,9'-dihexylfluorene and 2-(2,6-bis(4-(2-phenyl-2-cyanovinyl)-2,5-bis(hexyloxy)styryl)-4H-pyran-4-ylidene)malononitrile (**DCM**) were synthesized by the Suzuki coupling reaction. They were characterized by molecular weight determination, elemental analysis, FT-IR spectroscopy, DSC, TGA, absorption and emission spectroscopy, and cyclic voltammetry (CV). The copolymer films showed absorption peaks at 383–397 and 481–496 nm, and PL peaks at 421–424 and 560–596 nm originated from fluorene and **DCM** segments, respectively. The longer wavelength PL peak red-shifted gradually from 560 to 596 nm with increasing **DCM** contents (0.83%→49.8%). The LUMO energy levels lowered as the content of **DCM** units increased (−2.75 eV→−3.70 eV), whereas the HOMO levels remained almost unchanged (−5.68 eV→−5.64 eV). Electroluminescent devices, ITO/PEDOT:PSS/polymer/Ca(50 nm)/Al(150 nm), were fabricated to investigate the influence of **DCM** contents on emission characteristics. The maximum brightness and current efficiency of the **PFD0.5** device (1719 cd/m² and 0.25 cd/A) surpassed those of the **PF** device (1012 cd/m² 0.17 cd/A). With an increase in **DCM** content, the current efficiency was further increased to 0.30 cd/A at about 5% **DCM** units. The EL emission of **PFD5–PFD50** was exclusively originated from **DCM** fluorophores (>550 nm) due to rampant energy transfer. However, simultaneous emission of **PF** and **DCM** segments was readily obtained by lowering **DCM** contents (**PFD0.5**, **PFD1**, or by blending **PFD0.5** with **PF**).

Introduction

Conjugated polymers are of wide current interest for applications in electronic and optoelectronic devices including organic light-emitting diodes (OLEDs),^{1–3} thin film transistors,⁴ and photovoltaic cells.⁵ In the field of polymer-based electroluminescent (EL) devices, much interest has been paid to main-chain conducting polymers such as poly(phenylenevinylene) (PPV),^{1a} poly(*p*-phenylene) (PPP),⁶ poly(thiophene),⁷ poly(fluorene),⁸ their copolymers, and soluble derivatives because of potential application as large-area light-emitting diodes (LEDs). Poly(fluorene)s (PFs) with large band gaps have emerged as very promising materials for blue emission because of their unique combination of high thermal stability, high hole mobility, easy processability, and high photoluminescence (PL) quantum yield in the solid state.⁹ However, the major drawback of PFs is that they display a red-shifted and diminished emission upon thermal annealing or passage of current. The source of this long wavelength emission was initially believed to be excimer emission from aggregates formed by π -stacking of the polymer chains.¹⁰ Recently, the origin of the long wavelength emission, however, was ascribed to keto defects incorporated in the polymer backbone.^{9a,11} Numerous approaches have been adopted to suppress this undesired long wavelength emission: copolymerization with anthracene,¹² introduction of a “kink” disorder along the conjugated polymer chain,¹³ introduction of spirobi-fluorene into small compounds or polymeric chains,¹⁴ end-capping with sterically hindered group¹⁵ or hole trapping moiety,¹⁶ and introduction of bulky substituents at the 9-position of the fluorene unit.¹⁷

Blue-emitting PF is a p-type (electron donor, hole transport) material that transports holes with high mobility,^{9c,18} and electron injection and transport in PF is relatively poor. Our motivation

for the present work was to synthesize polyfluorenes with improved electron-injection and -transport characteristics by copolymerizing with an electron-deficient (n-type) building block. Meanwhile, the PF segment owns a large energy band, which would promote energy transfer to the other part with a lower band gap, leading to changes in electronic properties. In general, this method enables tunability of the luminescent colors. Also, fluorene-containing polymers have been shown to emit efficiently across the entire visible spectrum.¹⁹

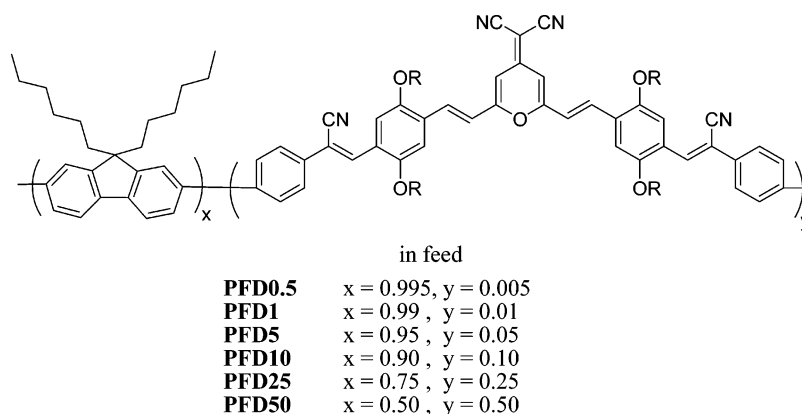
In this investigation, we designed and synthesized a series of fluorene copolymers (Chart 1) containing the **DCM**-derivatized moiety (0.5–50 mol % in feed), which are well-known low molecular weight red-emitting materials^{13b,20,21} from Eastman Kodak (**DCM** class). All of the **DCM** class red dyes contain 2-pyran-4-ylidene-malononitrile (PM) derivatives as electron acceptor. We attempted to extend the conjugation length and enhance the electron affinity of the copolymers by introducing the *p*-phenylenevinylene segment with a cyano group onto the vinylene unit. Additionally, the side *n*-hexyloxy groups were incorporated to increase the solubility of the copolymers. The PL emission changed gradually with the **DCM** contents in the copolymers, from yellow at low ratio to red at high ratio. Furthermore, we tried to find the optimal ratio of the **DCM** content in the copolymer or blend, which simultaneously contained the fluorene emission (blue) and the **DCM** emission (yellow), to obtain the white light. This article presents the synthesis and characterization of the new **DCM**-containing copolyfluorenes, followed by discussions of their photophysical, electrochemical, and electroluminescent properties.

Experimental Section

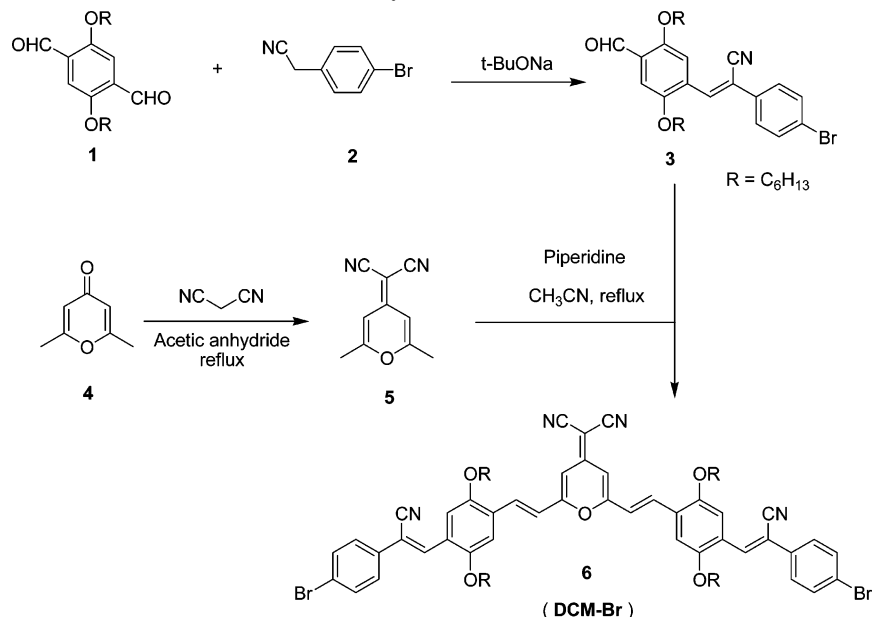
Materials and Measurement. All of the chemicals were purchased from Aldrich, Acros, TCI, and Lancaster Chemicals Co. and used without further purification. All of the solvents such as toluene, piperidine, and acetonitrile were dried with the appropriate

* Corresponding author. E-mail: yunchen@mail.ncku.edu.tw.

Chart 1



Scheme 1. Synthesis of Monomer 6



drying agents, then distilled under reduced pressure, and stored over 4 Å molecular sieves before use. The catalyst was tetrakis-(triphenylphosphine)palladium [Pd(PPh₃)₄] from Acros,²² and (2,6-dimethyl-4*H*-pyran-4-ylidene)propanedinitrile (**5**) was synthesized from 2,6-dimethyl-4-pyrone (**4**) and malononitrile by the method of Woods.²³ All new compounds were identified by ¹H NMR, FT-IR, and elemental analysis (EA). The ¹H NMR spectra were recorded with a Bruker AVANCE-300 or 400 NMR spectrometers, and chemical shifts are reported in ppm using tetramethylsilane (TMS) as an internal standard. The FT-IR spectra were measured as a KBr disk using a Fourier transform infrared spectrometer, model Jasco 7850. The elemental analysis was carried out on a Heraeus CHN-Rapid elemental analyzer. The molecular weight and molecular weight distribution of the copolymers were determined by a gel permeation chromatograph (GPC) using chloroform (CHCl₃) as eluent. Monodisperse polystyrene standards were used for calibration. The thermogravimetric analysis (TGA) of the polymers was performed under nitrogen atmosphere at a heating rate of 20 °C/min using a Perkin-Elmer TGA-7 thermal analyzer. Thermal transitions of the polymers were measured using a differential scanning calorimeter (DSC), Perkin-Elmer DSC-7, under nitrogen atmosphere at a heating rate of 10 °C/min. The glass-transition temperatures (*T*_g) were obtained from the second heating curve. Absorption spectra were measured with a Jasco V-550 spectrophotometer, and PL spectra were obtained using a Hitachi F-4500 fluorescence spectrophotometer. The cyclic voltammograms were recorded using a voltammetric analyzer (model CV-50W from BAS) at room temperature under nitrogen atmosphere. The measur-

ing cell consisted of polymer-coated Pt as working electrode, Ag/AgCl electrode as reference electrode, and platinum wire electrode as auxiliary electrode, supporting in 0.1 M (*n*-Bu)₄NClO₄ in acetonitrile. The energy levels were calculated using the ferrocene (FOC) value of -4.8 eV with respect to vacuum level, which is defined as zero.²⁴ The measured oxidation potential of ferrocene (*E*_{FOC}) (vs Ag/AgCl) was 0.46 V. Therefore, the HOMO level of the polymers could be calculated by the equation $E_{\text{HOMO}} = -e(E_{\text{onset(ox)}}) - 0.46 \text{ V} - 4.8 \text{ eV} = -e(E_{\text{onset(ox)}}) + 4.34 \text{ V}$, and the LUMO level could be estimated by the equation $E_{\text{LUMO}} = -e(E_{\text{onset(red)}}) + 4.34 \text{ V}$.

Synthesis of Monomers (Scheme 1). 4-[2-(4-Bromophenyl)-2-cyanovinyl]-2,5-bis(hexyloxy)benzaldehyde (**3**),²⁵ 2,5-Dihexyloxyterephthalaldehyde²⁶ (**1**: 1.00 g, 3.0 mmol) and 4-bromophenylacetonitrile (**2**: 0.650 g, 3.3 mmol) were dissolved in methanol (30 mL). The mixture was added to *t*-BuOK (17 mg, 0.15 mmol) under gentle stirring and allowed to react for 5 h at room temperature. The product was obtained as a precipitate, which was collected by filtration and washed with water. The solid was then recrystallized from *n*-hexane to give **3** (0.91 g, 59.4%); mp 91–92 °C. ¹H NMR (CDCl₃, 300 MHz, ppm): δ 10.49 (s, 1H, -CHO), 7.97 (s, 1H, =CH-), 7.86 (s, 1H, Ar-H), 7.61–7.50 (m, 4H, Ar-H), 7.34 (s, 1H, Ar-H), 4.17–3.96 (m, 4H, -OCH₂-), 1.90–1.66 (m, 4H, -CH₂-), 1.57–1.25 (m, 12H, -CH₂-), 0.93–0.89 (m, 6H, -CH₃). FT-IR (film, cm⁻¹): ν 3045, 2938, 2859 (-CHO), 2221 (-CN), 1684, 1484, 1209, 1035, 880, 819 (-C=CH-). Anal. Calcd for C₂₈H₃₄BrNO₃: C, 65.62%; H, 6.69%; N, 2.73%. Found: C, 65.17%; H, 7.07%; N, 2.79%.

Scheme 2. Synthesis of the Copolyfluorenes (PFDy)

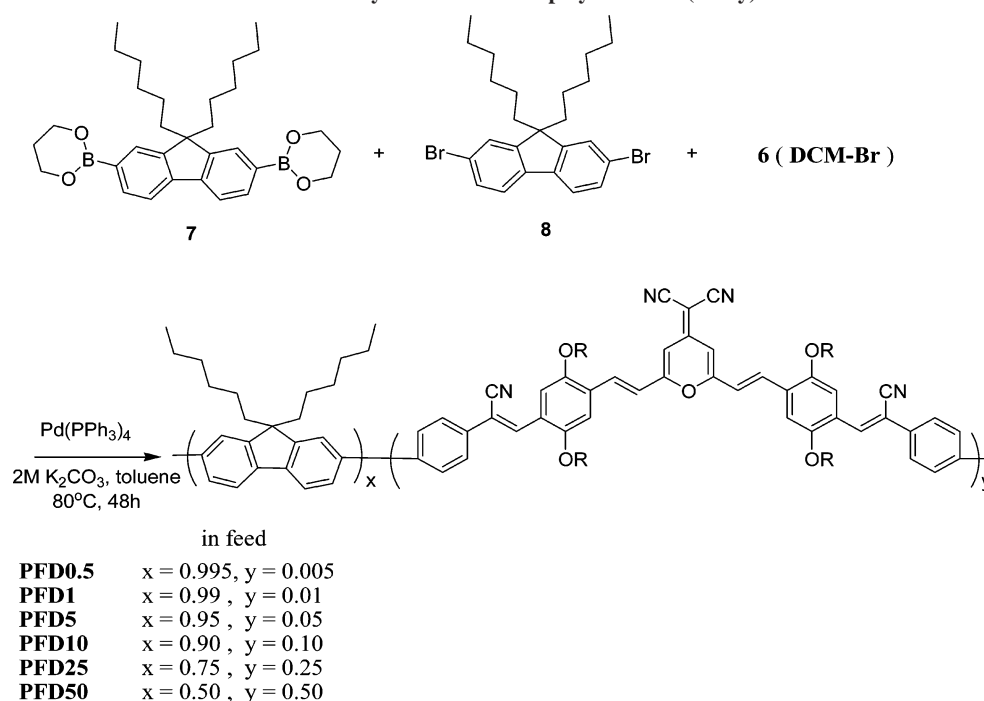


Table 1. Polymerization Results and Characterization of the Copolymers

| | M_n^a ($\times 10^4$) | M_w^a ($\times 10^4$) | PDI ^a | T_g (°C) | T_d (°C) ^b | y (%) ^c | $W_{R,air}$ (%) ^d |
|---------------|------------------------------|------------------------------|------------------|---------------|----------------------------|--------------------|---------------------------------|
| PFD0.5 | 3.57 | 7.69 | 2.15 | 100 | 433 | 0.83 | 3.8 (53.5) |
| PFD1 | 2.29 | 5.62 | 2.45 | 100.5 | 428 | 1.3 | 3.1 (52.4) |
| PFD5 | 1.25 | 2.36 | 1.89 | 103.4 | 423 | 5.6 | 5.1 (56.3) |
| PFD10 | 1.04 | 1.93 | 1.85 | | 421 | 11.6 | 3.9 (55.2) |
| PFD25 | 1.47 | 2.46 | 1.67 | | 415 | 28.4 | 2.3 (49.2) |
| PFD50 | 1.25 | 2.21 | 1.76 | | 416 | 49.8 | 2.6 (49.4) |

^a M_n , M_w , and PDI of the polymers were determined by gel permeation chromatography using polystyrene standards in CHCl_3 . ^b The temperature at 5 wt % loss under nitrogen atmosphere. ^c The y values were actual molar fraction of the DCM unit in the copolymers, as determined by elemental analysis (EA). ^d Residual weight: remaining weight of the sample upon heating to 800 °C in air; the values in the parentheses are those under nitrogen atmosphere.

(2,6-Dimethyl-4H-pyran-4-ylidene)propanedinitrile (**5**).²³ A mixture of 2,6-dimethyl-4-pyrone (**4**: 1.25 g, 10.06 mmol) and malononitrile (0.783 g, 11.85 mmol) in 5 mL of acetic anhydride was stirred and heated to 140 °C for 1 h under nitrogen atmosphere. The acetic acid was aspirated off, and the residue was washed with 10 mL of boiling water and collected by filtration to give brown material. Recrystallization from ethanol gave **5** (1.14 g, 65.8%); mp 192–195 °C. ¹H NMR (acetone- d_6 , 400 MHz, ppm): δ 6.60 (s, 2H, Ar-H), 2.41 (s, 6H, $-\text{CH}_3$). FT-IR (film, cm^{-1}): ν 2206 ($-\text{CN}$), 1666 ($-\text{C}=\text{C}-$), 1579, 1507, 1428 ($-\text{CH}_3$), 1336, 1276, 1176 ($\text{C}-\text{O}-\text{C}$), 920, 847. Anal. Calcd for $\text{C}_{10}\text{H}_8\text{N}_2\text{O}$: C, 69.76%; H, 4.68%; N, 16.27%. Found: C, 69.43%; H, 4.76%; N, 16.12%.

2-(2,6-Bis(4-(2-(4-bromophenyl)-2-cyanovinyl)-2,5-bis(hexyloxy)styryl)-4H-pyran-4-ylidene)malononitrile (**6**) (DCM-Br).²⁷ A mixture of **3** (0.615 g, 1.20 mmol), **5** (86 mg, 0.5 mmol), piperidine (5 drops), and freshly distilled acetonitrile (10 mL) was refluxed under nitrogen atmosphere for 24 h. The reaction mixture was cooled to room temperature, and the appeared precipitate was collected by filtration and washed with 50 mL of acetonitrile. The crude product was further washed with acetone to give **6** as an orange powder with a yield of 79%; mp 245–246 °C. ¹H NMR (acetone- d_6 , 400 MHz, ppm): δ 8.00 (s, 2H, Ar-H), 7.90 (s, 2H, $-\text{C}=\text{CH}-$), 7.89–7.85, 7 (d, $J = 16$ Hz, 2H, Ar-H), 7.60–7.54 (m, 8H, Ar-H), 7.06 (s, 2H, $-\text{C}=\text{CH}-$), 6.98–6.94 (d, $J = 16$ Hz, 2H, Ar-H), 6.72 (s, 2H, Ar-H), 4.16–4.05 (m, 8H,

Table 2. Photophysical Properties of the Copolymers

| | solution ^a | | | film | |
|---------------|---|--|----------------------|---|--|
| | absorption λ_{max} (nm) | PL λ_{max} (nm) ^b | Φ_{PL}^d | absorption λ_{max} (nm) | PL λ_{max} (nm) ^b |
| PFD0.5 | 388 | 419 (440) ^c | 0.93 | 389 | 424, 560 |
| PFD1 | 387 | 418 (441) | 0.73 | 389 | 422, 562 |
| PFD5 | 383, 478 | 418 (563) | 0.39 | 387, 481 | 422, 578 |
| PFD10 | 379, 479 | 418 (564) | 0.2 | 383, 486 | 422, 581 |
| PFD25 | 374, 478 | (415) 565 | 0.025 | 384, 489 | 421, 591 |
| PFD50 | 378, 478 | (417) 565 | 0.018 | 397, 496 | 421, 596 |

^a In chloroform (1×10^{-5} M). ^b The excitation wavelength was 380 nm. ^c The values in the parentheses are the PL λ_{max} of the minor peak or shoulder. ^d The PL efficiencies of the copolymers using **PF** as reference (assuming the Φ_{PL} of **PF** is 1).

$-\text{OCH}_2-$), 1.88–1.83 (m, 8H, $-\text{CH}_2-$), 1.53–1.21 (m, 24H, $-\text{CH}_2-$), 0.92–0.75 (m, 12H, $-\text{CH}_3$). FT-IR (film, cm^{-1}): ν 3063, 2935, 2206 ($-\text{CN}$), 1636, 1496, 1209, 1012, 827 ($-\text{C}=\text{CH}-$). Anal. Calcd for $\text{C}_{66}\text{H}_{72}\text{Br}_2\text{N}_4\text{O}_5$: C, 68.27%; H, 6.25%; N, 4.83%. Found: C, 68.30%; H, 6.55%; N, 4.89%.

Polymer Synthesis (Scheme 2).²⁸ Polymerization. The synthesis of polyfluorene (**PF**) (M_n , 14 200; M_w , 30 400; PDI, 2.13) and copolyfluorenes (**PFD0.5**–**PFD50**) was carried out using a palladium-catalyzed Suzuki coupling reaction. For instance, carefully purified 9,9-dihexylfluorene-2,7-bis(trimethylboronate) (**7**), 9,9-dihexyl-2,7-dibromofluorene (**8**), 2-(2-bis(4-(2-(4-bromophenyl)-2-cyanovinyl)-2,5-bis(hexyloxy)styryl)-4H-pyran-4-ylidene)malononitrile (**6**), and $(\text{PPh}_3)_4\text{Pd}(0)$ (0.5–1.5 mol %) were dissolved in a mixture consisting of toluene, an aqueous solution of K_2CO_3 (2 M), and ethanol. The mixture was first purged with nitrogen and allowed to react at 80 °C for 24–48 h under vigorous stirring. Next, **7** and 9,9-dihexyl-2-bromofluorene²⁹ were successively added to end-cap the polymer chain. The whole mixture was poured into a large excess of methanol and distilled water ($v/v = 10/1$). The resulted solid was collected by filtration and washed successively with methanol, distilled water, and then acetone, followed by Soxhlet extraction with acetone to remove oligomers and catalyst residues. The resulted polymers were soluble in conventional organic solvents such as toluene and chloroform. The contents of carbon, nitrogen, and hydrogen obtained from elemental analysis were used for the calculation of actual copolymer compositions. Anal. Found: for **PFD0.5**, C, 88.58%; N, 0.135%; H, 9.68%; for **PFD1**, C, 88.515%; N, 0.21%; H, 9.61%; for **PFD5**, C, 85.875%;

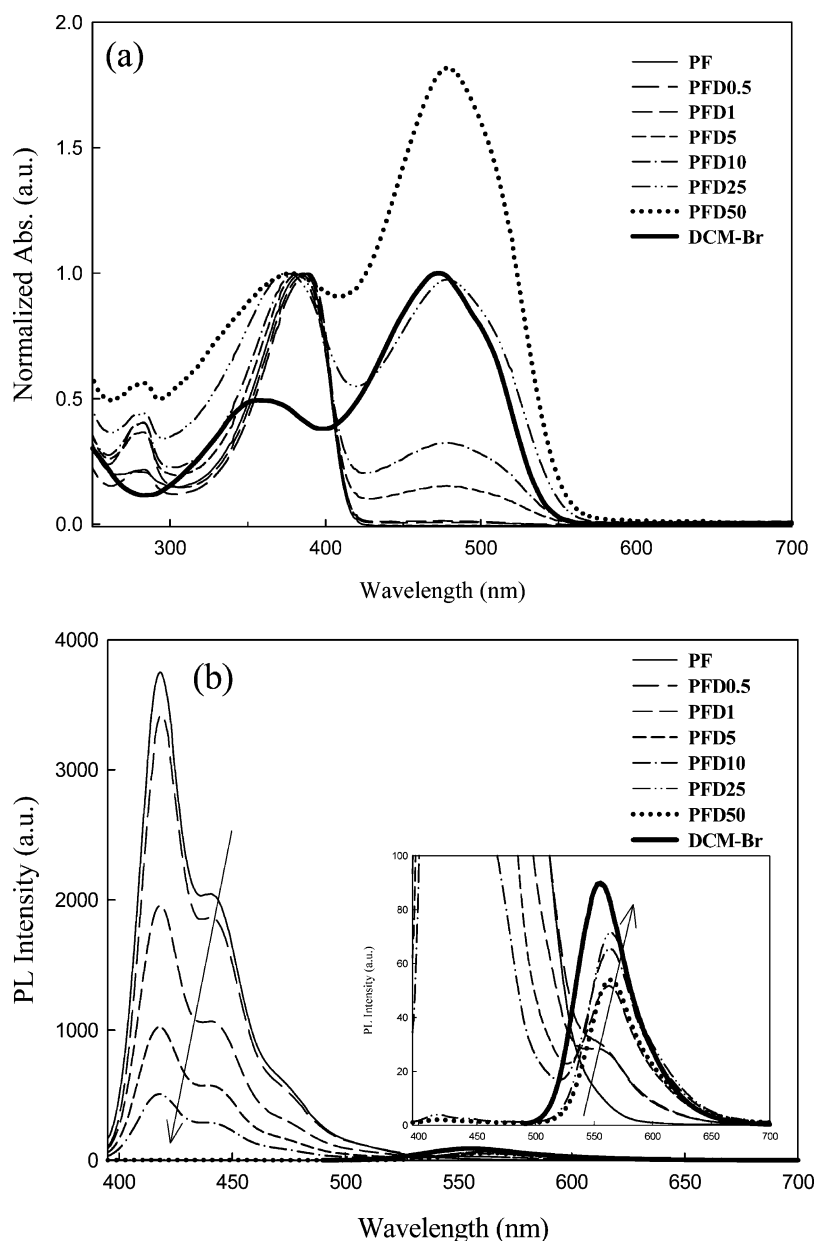


Figure 1. (a) Absorption and (b) PL spectra (excitation: 380 nm) of PF, PFD0.5–50, and DCM-Br (excitation: 473 nm) in chloroform (1×10^{-5} M).

N, 0.82%; H, 9.21%; for **PFD10**, C, 84.725%; N, 1.535%; H, 8.89%; for **PFD25**, C, 82.455%; N, 2.98%; H, 8.33%; for **PFD50**, C, 80.58%; N, 4.125%; H, 7.81%.

Fabrication of LED Devices. Double layer light-emitting diodes (ITO/PEDOT:PSS/polymer/Ca/Al) were fabricated for the investigation of optoelectronic characteristics. The ITO-coated glasses were cleaned sequentially in ultrasonic baths of a neutraler reiniger/deionized water (1:10 volume) mixture, deionized water, acetone, and 2-propanol, and then dried in a vacuum overnight. A thick hole-injection layer of PEDOT:PSS was spin-coated on top of ITO-coated glasses and dried at 150 °C for 15 min under a vacuum. The emitting layer was then spin-coated onto the PEDOT layer from a polymer solution in toluene or chloroform, followed by drying in a vacuum overnight. The concentration of the polymer solution was 1 wt % and filtered through a 0.2 μ m syringe filter before spin-coating. Finally, a thick layer of Ca and Al electrodes was vacuum-deposited using a VPC-060 (ULVAC) vacuum coater at the pressure of 10^{-6} Torr. Device luminance, EL spectra, and current–voltage characteristics were recorded using a combination of Keithley power supply (model 2400) and Ocean Optics usb2000 fluorescence spectrophotometer. All of the fabrication and char-

acterization of the light-emitting diode devices was performed in air and at room temperature without protective encapsulation.

Results and Discussion

Synthesis and Characterization. Synthetic routes employed for the preparation of monomer and polymers are shown in Schemes 1 and 2, respectively. The reaction of compound **1** with **2** afforded mainly mono-vinylene derivative (**3**). The reaction was conducted under room temperature with the *t*-BuOK being added slowly in several portions to suppress the formation of divinylene derivative. Also, the trace divinylene derivative was completely removed by recrystallization. The monomer **6** was prepared through Knoevenagel condensation between **3** and **5** in a yield over 79%. The polymerization reaction was proceeded by the well-known palladium-catalyzed Suzuki coupling reaction between 9,9-dihexylfluorene-2,7-bis-(trimethyleneborate) (**7**) and functionalized dibromo aromatic monomers **6** (DCM-Br) and **8**.³⁰ The molar percents of **6** in the feed were between 0.5 and 50 as shown in the numbers after PFD. The copolymers PFD0.5–PFD10 are soluble in

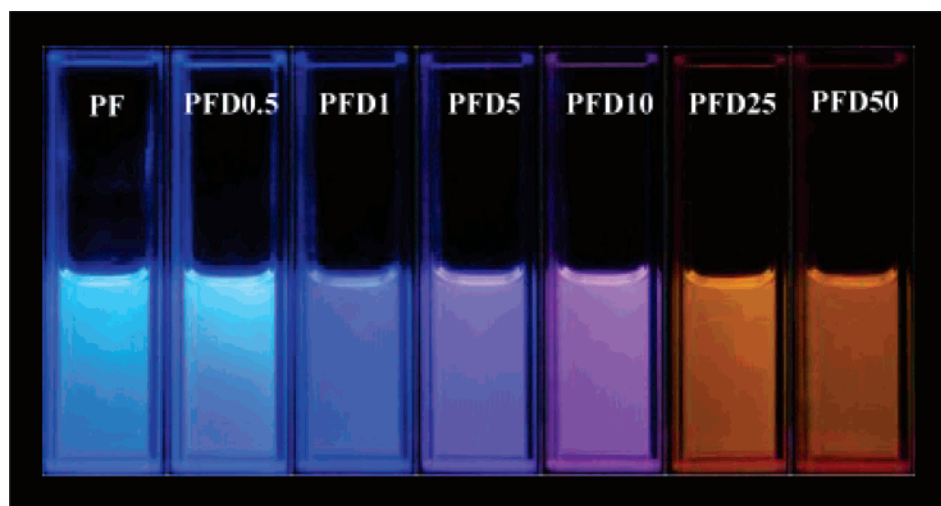


Figure 2. Photoluminescence of the polymer solutions (1×10^{-5} M in chloroform) under irradiation with 365 nm light.

common organic solvents such as chloroform, toluene, xylene, and dichloromethane. However, with an increase in **DCM** content the copolymers **PFD25** and **PFD50** are soluble only in chloroform and dichloromethane, indicating that their solubility seems to decrease with increasing **DCM** contents. Their molecular weights were determined by gel permeation chromatography using monodisperse polystyrene as the calibration standard. As shown in Table 1, the weight-average molecular weights (M_w) are $(1.93\text{--}7.69) \times 10^4$ with the polydispersity indexes (PDI) lying around 1.67–2.45. The actual compositions of these copolymers were estimated from the data of elemental analysis, and the mole percents of **DCM** unit were 0.83, 1.3, 5.6, 11.6, 28.4, and 49.8, respectively. The mole percents of **DCM** moiety are slightly greater than those of feed composition (0.5, 1, 5, 10, 25, 50 mol %) except for **PFD50**, suggesting that the **DCM** monomer (**6**) exhibits a higher reactivity than does the 2,7-dibromofluorene monomer (**8**).

Thermal properties of the polymers were evaluated by thermogravimetric analysis (TGA) and a differential scanning calorimeter (DSC), and the results are summarized in Table 1. Their onset decomposition temperatures (at 5 wt % loss) and residual weights ($W_{R,air}$) under nitrogen atmosphere are in the range of 415–433 °C and 49.2–56.3%, respectively, indicating that the copolymers are quite stable at elevated temperature. The residual weights of **PFD0.5–50** at 800 °C in air were 3.8%, 3.1%, 5.1%, 3.9%, 2.3%, and 2.6%, respectively. Therefore, the copolymers are almost burnt away at high temperature, suggesting that the actual compositions of these copolymers can be properly estimated from the data of elemental analysis. The glass-transition temperatures (T_g) of the polymers obtained by DSC were 100 °C for **PFD0.5**, 100.5 °C for **PFD1**, and 103.4 °C for **PFD5**, which are higher than 97 °C for **PF**.^{13b} However, the glass transition temperature of **PFD10**, **PFD25**, and **PFD50** could not be clearly identified on their thermograms. It is obvious that the incorporation of **DCM** moiety slightly increases the T_g value, which is possibly due to reduced segmental motions as well as more dense packing in polymer main chains. High T_g is very important for such types of polymers when used as emissive materials in PLEDs.³¹

Photophysical Properties. The photophysical characteristics of the copolymers were investigated both in CHCl_3 and as films cast from solution. Their absorption and emission spectral data are summarized in Table 2. Figure 1 displays the absorption and photoluminescence (PL) spectra of **PF**, **PFDs**, and **DCM-Br** in dilute solution (1×10^{-5} M). All of the polymers show

the major and maximum absorption in the range 374–388 nm, which can be attributed to $\pi\text{--}\pi^*$ transitions of main-chain π -conjugated system.³² In addition, the copolymers, except for **PFD0.5** and **PFD1**, exhibit a longer wavelength absorption in the range 478–479 nm, which should be originated from the **DCM** chromophores because its position is almost co-incident with that of **DCM-Br**. Moreover, the absorption spectra exhibit a gradual blue-shift with an increase in **DCM** fractions, that is, from 388 nm in **PFD0.5** to 374 nm in **PFD25**. The gradual blue-shift can be justified by random interruption of π -conjugation in the backbone after incorporating the **DCM** unit.^{13a} Additionally, accompanied by increasing **DCM** content, the intensity of longer wavelength absorption is progressively raised relative to the absorption maximum at 374–388 nm. When the **DCM** content reaches 50% (**PFD50**), the absorption spectrum shows great resemblance to that of **DCM-Br**. It is suggested that the **DCM** unit is not involved in the main-chain conjugation system and possesses its own localization π -system. Consequently, the absorption peak position of the **DCM** moiety (478–479) is rather independent of its content in the polymers.

Figure 1b shows the PL spectra of the polymers obtained in dilute chloroform solution (excitation wavelength 380 nm). The emission spectrum of **PF** exhibits typical vibronic progression with the 0–0 PL emission band situated at 417 nm and the 0–1 transition at 440 nm. The copolymers (**PFDs**) also display two characteristic emission bands at about 415–419 and 563–565 nm.³³ The shorter wavelength emission originates from fluorene segments, while the longer wavelength one (563–565 nm) comes from the **DCM** moiety. The PL spectral intensity depends strongly on the concentration of **DCM** chromophores; for instance, the emission of fluorene segments around 417 nm degenerates quickly with increasing **DCM** contents. On the contrary, the emission intensity of **DCM** chromophores at ca. 563–565 nm (as shown in inset) enhances obviously with increasing **DCM** contents. This is attributable to excited energy transfer from fluorene segments to **DCM** units, which become more prevalent at high **DCM** ratios. Depending on the contents of **DCM** moiety, variable color photoluminescence can be observed under irradiation with a general UV lamp ($\lambda = 365$ nm) as shown in Figure 2. The PL efficiencies of the copolymers, using **PF** as the reference, are 0.97, 0.73, 0.39, 0.2, 0.025, and 0.018 (Table 2), respectively, and they obviously reduce with increasing **DCM** content. This is attributable to the interruption of main-chain conjugation by the **DCM** units.

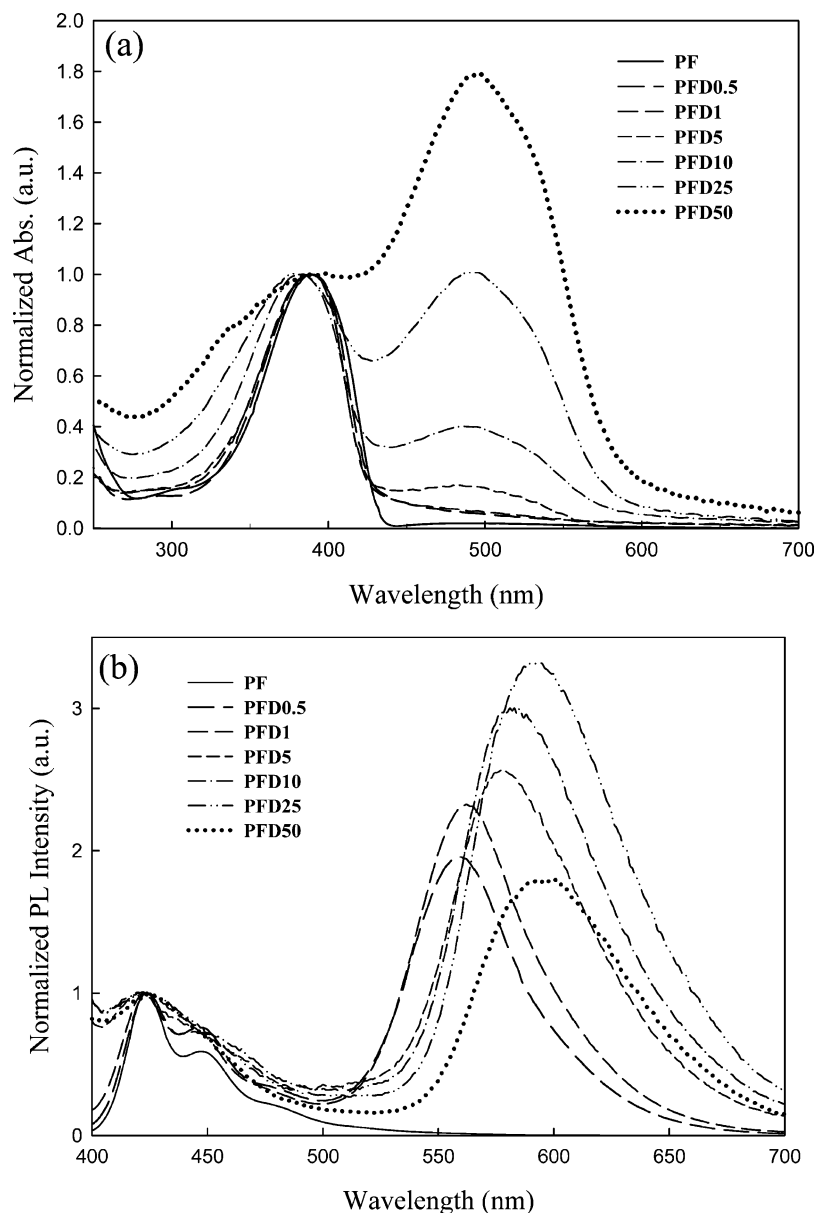


Figure 3. (a) Absorption and (b) PL spectra of **PFD0.5–50** in the film state (excitation wavelength: 380 nm).

Figure 3 shows the absorption and PL spectra in the film state. The absorption spectra in the film state are similar to those in the solution state (Figure 1), except that there are 1–19 and 3–18 nm red-shifts for fluorene and **DCM** units, respectively. As shown in Figure 3b, all of the copolymers reveal both emission from fluorene segments ($\lambda_{\text{max}} = 421\text{--}424$ nm) and the longer wavelength emission from the **DCM** moieties ($\lambda_{\text{max}} = 560\text{--}596$ nm). The relative PL intensity of the longer wavelength emission is enhanced with increasing **DCM** concentration (except **PFD50**) and is stronger than that of shorter wavelength emission. These results can be attributed to easier exciton migration or energy transfer from the fluorene segments to the **DCM** moieties in the film state, which make the longer wavelength emission in the film state more obvious than that in the solution state. However, the intensity of longer wavelength emission abruptly diminishes for **PFD50**. This is probably due to the fact that **PFD50** is an alternate copolymer in which the conjugation of the fluorene segments is completely interrupted by the **DCM** units. Greatly reduced absorption of **PFD50** at 380 nm (excitation wavelength) leads to an abrupt decrease in its PL intensity. However, the concentration quenching effect between **DCM** moieties cannot be neglected either.³⁴ Further-

more, with the increase of **DCM** concentration, the emission spectrum of fluorene segments (around 422 nm) gradually loses its well-resolved structure. This can be attributed to lack of intrachain ordering due to the overwhelming kinks in the backbone, which has also been observed in the polyfluorene–quinoxaline system reported by Kullarni et al.³⁵

Moreover, with an increase in **DCM** fractions, the PL emission peak gradually shifts from 560 to 596 nm. This is possibly due to aggregate formation between **DCM** chromophores at higher **DCM** concentration. To further demonstrate that the aggregation occurred in high concentration of the **DCM** unit, blend films were prepared from **PF** and **PFD25** to investigate PL spectral variations. Figure 4 shows the PL spectra of the blend films containing the different ratios of the **PF** and **PFD25**. For instance, the molar percentage of the **DCM** unit is 1% in the blend (designated as blend 1%) if the ratio of **PF** to **PFD25** is 24:1. Similar to the behavior observed for the copolymers, the PL spectra of the polymer blends show a gradual red-shift with an increase in **DCM** concentration (from 0.05 to 20 mol %); that is, emission maximum shifts bathochromically from 539 nm (0.05 mol % **DCM**) to 595 nm (20 mol % **DCM**). Therefore, the red-shift is ascribed to aggregates

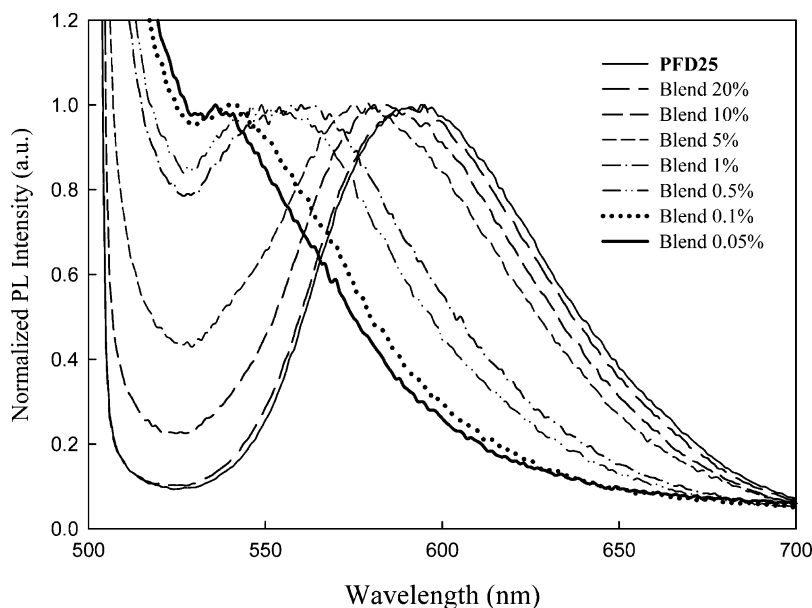


Figure 4. PL spectra of the blend film from **PF** and **PFD25** (excited by 500 nm). The values are the molar percent of **DCM** units in the blends.

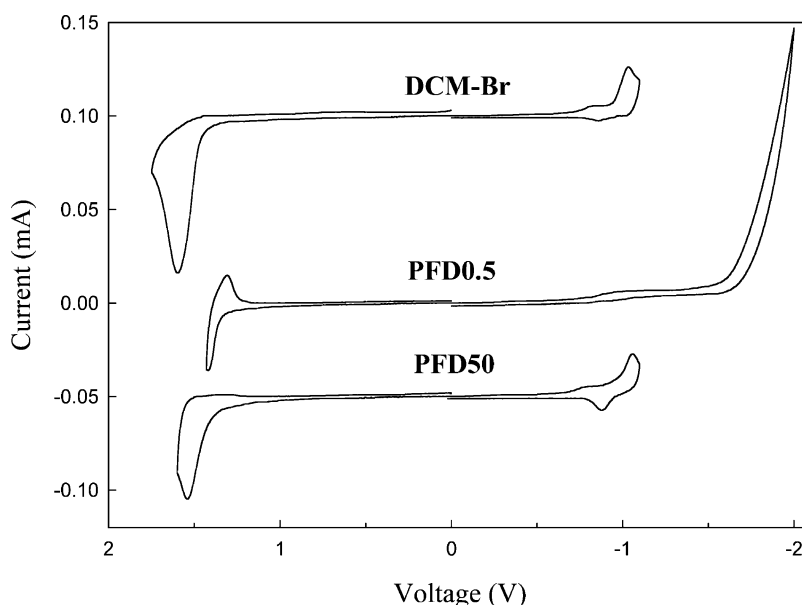


Figure 5. Cyclic voltammograms of **DCM**, **PFD0.5**, and **PFD50** films coated on Pt electrode (scan rate: 100 mV/s).

formed by the stacking of **DCM** moieties. Accordingly, the emission wavelength is mainly dependent upon the **DCM** content in the copolymers or the blends.

Electrochemical Properties. Cyclic voltammetry (CV) has been employed and considered as an effective tool in investigating electrochemical properties of conjugated compounds.³⁴ From the onset oxidation and reduction potentials in the cyclic voltammogram, the highest occupied molecular orbital (HOMO) and lowest unoccupied molecular orbital (LUMO) levels can be readily estimated, which correspond to ionization potential (IP) and electron affinity (EA), respectively. Polymer-coated Pt was used as working electrode, supporting in 0.10 M tetrabutylammonium perchlorate (Bu_4NClO_4) in anhydrous acetonitrile. Typical cyclic voltammograms of **DCM-Br**, **PFD0.5**, and **-50** in anodic and cathodic scan are shown in Figure 5 with related electrochemical data summarized in Table 3. The onset oxidation potentials are situated at 1.40–1.30 V for **DCM-Br**, **PF**, and **PFD0.5–50**, from which their HOMO levels are estimated to be -5.74 to -5.64 eV, respectively, according to the equation $\text{IP} = -(E_{\text{onset(ox)}} + 4.34)$ eV. Besides, the onset

Table 3. Electrochemical Potentials of the Copolymers and **DCM-Br**

| | $E_{\text{onset(ox)}} \text{ vs } \text{Ag}/\text{Ag}^+ \text{ (V)}^a$ | $E_{\text{onset(red)}} \text{ vs } \text{Ag}/\text{Ag}^+ \text{ (V)}^b$ | $E_{\text{HOMO}} \text{ (eV)}^c$ | $E_{\text{LUMO}} \text{ (eV)}^c$ | $E_{\text{g}}^{\text{el}} \text{ (eV)}^d$ |
|---------------|--|---|----------------------------------|----------------------------------|---|
| DCM-Br | 1.40 | −0.66 | −5.74 | −3.68 | 2.06 |
| PF | 1.34 | −1.59 | −5.68 | −2.75 | 2.93 |
| PFD0.5 | 1.34 | −1.59 | −5.68 | −2.75 | 2.93 |
| PFD1 | 1.34 | −1.59 | −5.68 | −2.75 | 2.93 |
| PFD5 | 1.30 | −1.59 | −5.64 | −2.75 | 2.89 |
| PFD10 | 1.30 | −1.59 | −5.64 | −2.75 | 2.89 |
| PFD25 | 1.30 | −0.66 | −5.64 | −3.68 | 1.96 |
| PFD50 | 1.30 | −0.64 | −5.64 | −3.70 | 1.94 |

^a Onset oxidation potential measured by cyclic voltammetry. ^b Onset reduction potential measured by cyclic voltammetry. ^c $E_{\text{HOMO}} = -e(E_{\text{onset(ox)}} + 4.34 \text{ V})$; $E_{\text{LUMO}} = -e(E_{\text{onset(red)}} + 4.34 \text{ V})$. ^d Band gaps obtained from electrochemical data.

reduction potentials of **DCM-Br**, **PF**, and **PFD0.5–50** are in the range of -1.59 to -0.64 V, with their LUMO levels estimated to be -3.70 to -2.75 eV according to the equation $\text{EA} = -(E_{\text{onset(red)}} + 4.34)$ eV. From the HOMO and LUMO levels, the band gaps of the copolymers were estimated to be 2.93, 2.93, 2.89, 2.89, 1.96, and 1.94 eV, respectively. It is

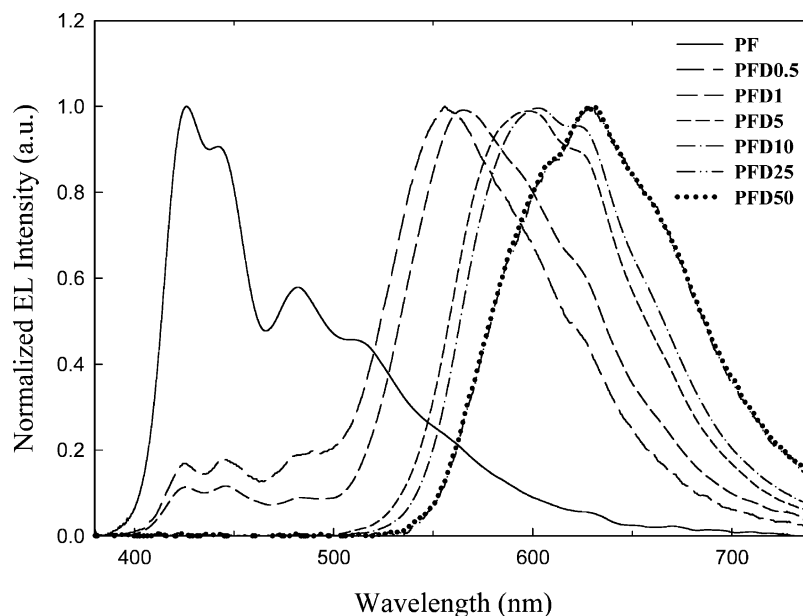


Figure 6. Electroluminescence spectra of the devices (ITO/PEDOT:PSS/polymer/Ca/Al).

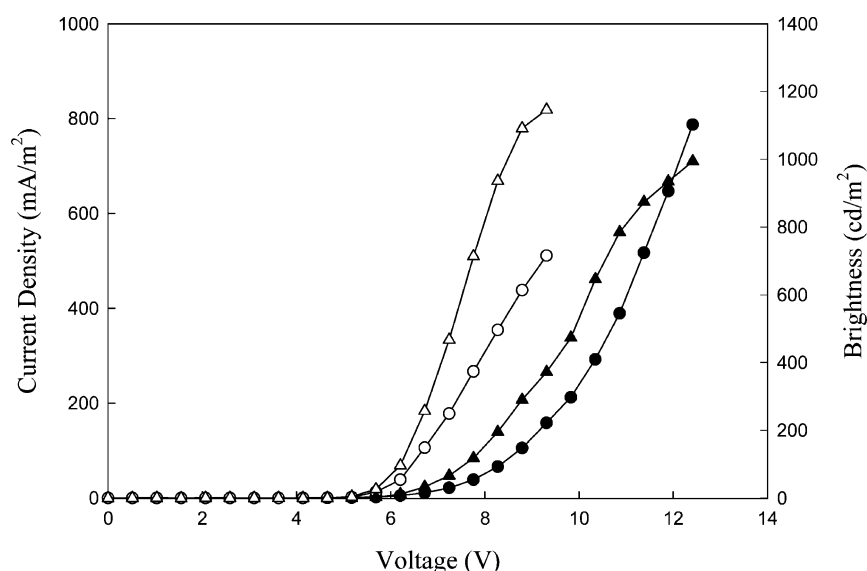


Figure 7. Current density–voltage (●, PFD5; ○, Blend-20) and brightness–voltage (▲, PFD5; △, Blend-20) characteristics of the EL devices.

noteworthy that the **DCM-Br** is a red-emitting chromophore with a small band gap ($E_g = 2.06$ eV). Furthermore, the LUMO level of the **DCM-Br** unit is very low (-3.68 eV), which is beneficial in promoting electron-transfer properties when incorporated in the copolymers. The results show that all of the copolymers have similar HOMO levels (-5.68 to -5.64 eV), suggesting that oxidation starts at fluorene segments regardless of the **DCM** contents (HOMO of **PF** = -5.7 eV). However, although the LUMO levels of **PFD0.5**–**PFD10** are the same (-2.75 eV), those of **PFD25** and **PFD50** are much lower (-3.68 to -3.70 eV). High LUMO levels in **PFD0.5**–**PFD10** are due to their low content of the **DCM** unit that makes the reduction start at fluorene segments.

Electroluminescent Properties of LED Devices. Double-layer electroluminescent devices using the polymers as emitting materials [ITO/PEDOT/polymer/Ca (50 nm)/Al (150 nm)] were fabricated to investigate their optoelectronic characteristics. Figure 6 shows the EL spectra of the devices. The major emission peak of the **PF** device is situated at 426 nm, which is similar to that in the PL spectra. The minor emission peak at 480 and one shoulder at 508 correspond to $S_{10} \rightarrow S_{02}$ and $S_{10} \rightarrow S_{03}$

Table 4. Electroluminescent Properties of the Devices

| device | V_{on}^a (V) | L_{max}^b (cd/m ²) | emission (λ_{em} , nm) | current efficiency ^c (cd/A) | (x , y) ^d |
|-----------------------|-------------------|-------------------------------------|------------------------------------|--|----------------------------|
| PF | 5.6 | 1012 | 426 | 0.17 | (0.18, 0.13) |
| PFD0.5 | 6.2 | 1719 | 425, 444, 555 | 0.25 | (0.40, 0.42) |
| PFD1 | 6.2 | 910 | 423, 565 | 0.23 | (0.45, 0.42) |
| PFD5 | 6.7 | 994 | 597 | 0.30 | (0.57, 0.42) |
| PFD10 | 6.6 | 961 | 603 | 0.17 | (0.58, 0.40) |
| PFD25 | 6.7 | 825 | 627 | 0.12 | (0.62, 0.37) |
| PFD50 | 6.5 | 639 | 631 | 0.086 | (0.62, 0.37) |
| Blend-20 ^e | 5.6 | 1146 | 425, 448, 485, 551 | 0.26 | (0.33, 0.35) |
| Blend-10 ^e | 6.6 | 1045 | 425, 449, 486, 550 | 0.27 | (0.32, 0.34) |
| Blend-5 ^e | 5.6 | 926 | 426, 449, 483, 548 | 0.25 | (0.24, 0.20) |

^a Turn-on voltage at 10 cd/m². ^b Luminance at maximum bias voltage.

^c Maximum current efficiency. ^d The 1931 CIE coordinate. ^e EL devices using blends of **PFD0.5** and **PF** as emitting layer; the values are molar percents of **PFD0.5** in the blends.

vibronic transition, respectively.³⁶ However, the EL spectra of **PFD** devices are very different from that of **PF**. In EL spectra of **PFD0.5** and **01**, for instance, the emission from fluorene segments ($\lambda_{em} = 426$ nm) degenerates significantly, and a very

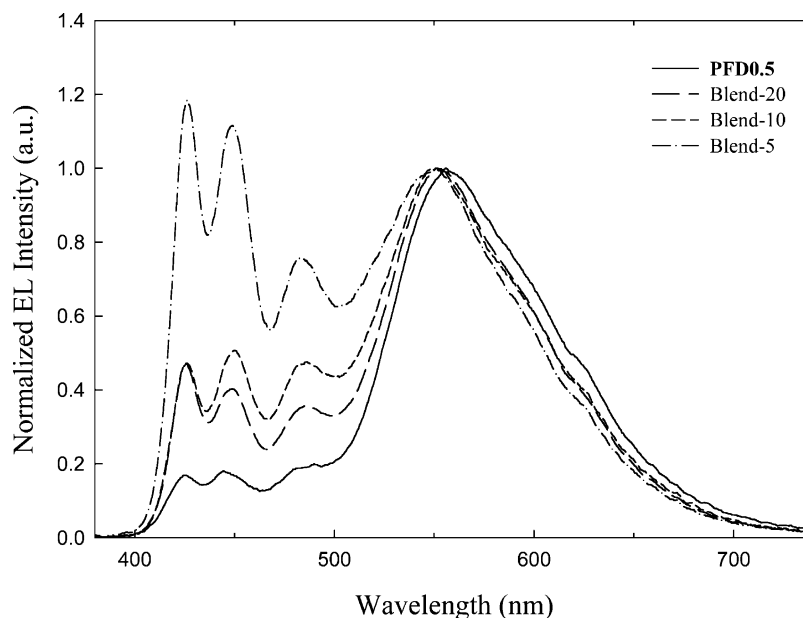


Figure 8. Emission spectra of the EL devices from **PFD0.5**, Blend-20, Blend-10, and Blend-5. The values after the hyphen are the molar percent of **PFD0.5** in the blends (**PF** + **PFD0.5**).

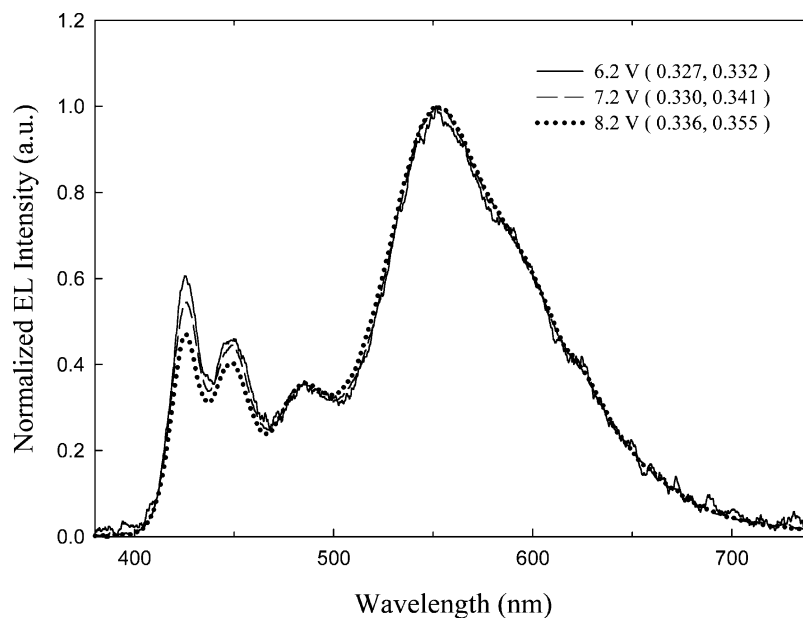


Figure 9. Electroluminescence spectra of Blend-20 device under different operating voltages. The values in the parentheses are the 1931 CIE coordinates (x , y) of the emission light.

intensive emission appears around 500–700 nm attributed to the **DCM** segments. However, the EL spectra of **PFD5**–**PFD50** exhibit exclusively the longer wavelength emission band ($\lambda_{\text{em}} = 597$ – 631 nm), which are mainly originated from **DCM** units. This indicates that excited energy transfers efficiently from fluorene segments to **DCM** units due to the smaller band gap of the **DCM** units. Furthermore, with an increase in **DCM** ratios, the emission peak (λ_{em}) red-shifts progressively from 555 to 631 nm, a tendency similar to that observed in their PL spectra. The red-shifted emission peaks are ascribed to excimers formed via intra- and/or intermolecular interactions.

Figure 7 shows the brightness and current density versus bias characteristics of the EL device from **PFD5**, and the related characteristic data of all EL devices are summarized in Table 4. The turn-on voltages (at 10 cd/m²) of the EL devices are in the range of 5.6–6.7 V, and the maximal brightness and current efficiency are 639–1719 cd/m² and 0.086–0.3 cd/A, respec-

tively. Specifically, the maximal brightness and current efficiency of the **PFD0.5** device are 1719 cd/m² and 0.25 cd/A, respectively, which surpass those of the **PF** device (1012 cd/m², 0.17 cd/A). With an increase in **DCM** content, for instance, in **PFD1** and **PFD5** devices, the current efficiency is enhanced further to 0.30 cd/A, although the maximum brightness drops slightly to 910 cd/m².

It is clear that white light emitting EL device is hard to obtain using **PFD0.5**–**50** due to rampant energy transfer. However, blending of **PFD0.5** with polyfluorene (**PF**) seems to be a good strategy because dilution of **DCM** chromophore not only enhances its dispersion but also diminishes energy transfer from fluorene segments. This will lead to simultaneous emission of both fluorophores. Figure 8 shows the EL spectra of blend devices Blend-20, Blend-10, and Blend-5, in which the values are the molar percents of **PFD0.5** in the blends. The emission spectral features of the blend devices are similar to that of

PFD0.5, but the peak intensity between 400 and 500 nm varies significantly. The EL emission wavelength of the **DCM** units is situated around 550 nm, while those of the fluorene moiety (425, 448, and 485 nm) enhance obviously with decreasing **DCM** contents (Blend-20→Blend-5). Accordingly, the 1931 CIE coordinates of the blend devices vary with the content of **DCM** units and are (0.33, 0.35) for Blend-20, (0.32, 0.34) for Blend-10, and (0.24, 0.20) for Blend-5, respectively (Table 4). The 1931 CIE coordinates of Blend-20 and Blend-10 considerably approach (0.33, 0.33) of white light. This is attributed to the obvious $S_{10} \rightarrow S_{02}$ and $S_{10} \rightarrow S_{03}$ vibronic transitions of the fluorene moieties and the broad emission from **DCM** moieties, which make the EL spectra broader than expected. The brightness and current density versus bias characteristics of the devices of Blend-20 are shown in Figure 7. The EL spectra of Blend-20 clearly reveal steady emission under different operating voltages (6.2–8.2 V), in which the CIE coordinate changes slightly from (0.327, 0.332) at 6.2 V to (0.336, 0.355) at 8.2 V, as shown in Figure 9. Present results suggest that blends of **PFD** and **PF** are potential materials for white light emission devices.

Conclusion

Copolyfluorenes containing **DCM** derivatives (0.83–49.8 mol %) have been successfully synthesized by the palladium-catalyzed Suzuki coupling reaction. They exhibited moderately high glass transition temperatures (>100 °C) and good thermal stability ($T_d > 410$ °C). In dilute solution, two major absorptions (374–388 and 478–479 nm) and two emission bands (415–419 and 563–565 nm) were attributed to fluorene segments and **DCM** units, respectively. In the film state, the emission maximum originated from **DCM** segments gradually shifted from 560 to 596 nm, as the fraction of the **DCM** units was increased. The copolymers showed similar HOMO levels (–5.68 to –5.64 eV), but the LUMO levels lowered gradually (–2.75→–3.70 eV) with increasing **DCM** units. In the EL spectra of **PFD5**–**PFD50** devices, the emission maxima were situated 597–631 nm originated mainly from **DCM** units. However, both emissions of **PF** and **DCM** were observed in **PFD0.5** and **PFD1**. The maximum brightness and current efficiency of **PFD0.5** devices were 1719 cd/m² and 0.25 cd/A, respectively, which surpassed those of the neat **PF** device (1012 cd/m², 0.17 cd/A). With an increase of **DCM** content, for instance, in **PFD1** and **PFD5** devices, the current efficiency was enhanced further to 0.30 cd/A. Moreover, the EL devices of blends from **PF** and **PFD0.5** exhibited near white light emission; that is, the CIE coordinates were (0.33, 0.35) and (0.32, 0.34) for Blend-20 and Blend-10, respectively. Moreover, the EL device of Blend-20 clearly revealed steady emission under different operating voltages (6.2–8.2 V). Current results suggest that blends of **PFD** and **PF** are potential emitting materials for white light devices.

Acknowledgment. We thank the National Science Council of the Republic of China for financial aid through project NSC 95-2221-E006-226-MY2.

References and Notes

- (1) (a) Burroughes, J. H.; Bradley, D. D. C.; Brown, A. R.; Marks, R. N.; Mackay, K.; Friend, R. H.; Burn, P. L.; Holmes, A. B. *Nature (London)* **1990**, *347*, 539. (b) Yang, Y.; Heeger, A. J. *Nature (London)* **1994**, *372*, 344. (c) Friend, R. H.; Gymer, R. W.; Holmes, A. B.; Burroughes, J. H.; Marks, R. N.; Taliani, C.; Bradley, D. D. C.; dos Santos, D. A.; Bredas, J. L.; Logdlund, M.; Salaneck, W. R. *Nature (London)* **1999**, *397*, 121. (d) Cao, Y.; Parker, I. D.; Yu, G.; Zhang, C.; Heeger, A. J. *Nature (London)* **1999**, *397*, 414.
- (2) (a) Zhang, X.; Shetty, A. S.; Jenekhe, S. A. *Macromolecules* **1999**, *32*, 7422. (b) Zhang, X.; Jenekhe, S. A. *Macromolecules* **2000**, *33*, 2069. (c) Liao, L.; Pang, Y.; Ding, L.; Karasz, F. E. *Macromolecules* **2001**, *34*, 7300. (d) Jenekhe, S. A.; Lu, L.; Alam, M. M. *Macromolecules* **2001**, *34*, 7315.
- (3) (a) Zhang, X.; Kale, D. M.; Jenekhe, S. A. *Macromolecules* **2002**, *35*, 382. (b) Zhu, Y.; Alam, M. M.; Jenekhe, S. A. *Macromolecules* **2002**, *35*, 9844. (c) Zhu, Y.; Alam, M. M.; Jenekhe, S. A. *Macromolecules* **2003**, *36*, 8958. (d) Yang, J.; Jiang, C.; Zhang, Y.; Yang, R.; Yang, W.; Hou, Q.; Cao, Y. *Macromolecules* **2004**, *37*, 1211. (e) Lu, J.; Tao, Y.; D'iorio, M.; Li, Y.; Ding, J.; Day, M. *Macromolecules* **2004**, *37*, 2442. (f) Tonzola, C. J.; Alam, M. M.; Bean, B. A.; Jenekhe, S. A. *Macromolecules* **2004**, *37*, 3554.
- (4) (a) Ong, B. S.; Wu, Y.; Liu, P.; Gardner, S. J. *Am. Chem. Soc.* **2004**, *126*, 3378–3379. (b) Babel, A.; Jenekhe, S. A. *J. Phys. Chem. B* **2003**, *107*, 1749–1754. (c) Babel, A.; Jenekhe, S. A. *Adv. Mater.* **2002**, *14*, 371.
- (5) (a) Brabec, C. J.; Sariciftci, N. S.; Hummelen, J. C. *Adv. Funct. Mater.* **2001**, *11*, 15. (b) Jenekhe, S. A.; Y, S. *Appl. Phys. Lett.* **2000**, *77*, 2635.
- (6) Grem, G.; Leditzky, G.; Ullrich, B.; Leising, G. *Adv. Mater.* **1992**, *4*, 36.
- (7) Andersson, M. R.; Thomas, O.; Mammo, W.; Svensson, M.; Theander, M.; Inganäs, O. *J. Mater. Chem.* **1999**, *9*, 1933.
- (8) Pei, Q.; Yang, Y. *J. Am. Chem. Soc.* **1996**, *118*, 7416.
- (9) (a) Scherf, U.; List, E. J. W. *Adv. Mater.* **2002**, *14*, 477. (b) Becker, S.; Ego, C.; Grimsdale, A. C.; List, E. J. W.; Marsitzky, D.; Pogantsch, A.; Setayesh, S.; Leising, G.; Müllen, K. *Synth. Met.* **2002**, *125*, 73. (c) Babel, A.; Jenekhe, S. A. *Macromolecules* **2003**, *36*, 7759.
- (10) (a) Pannozzo, S.; Vial, J.-C.; Kervalla, Y.; Stéphan, O. *J. Appl. Phys.* **1995**, *240*, 373. (b) Zeng, G.; Yu, W. L.; Chua, S. J.; Huang, W. *Macromolecules* **2002**, *35*, 6907.
- (11) (a) List, E. J. W.; Guentner, R.; Freitas, P. S. D.; Scherf, U. *Adv. Mater.* **2002**, *14*, 374. (b) Zhao, W.; Cao, T.; White, J. M. *Adv. Funct. Mater.* **2004**, *14*, 785.
- (12) Klarner, G.; Davey, M. H.; Chen, W. D.; Miller, R. D. *Adv. Mater.* **1998**, *10*, 993.
- (13) (a) Xia, C.; Advincula, R. C. *Macromolecules* **2001**, *34*, 5854. (b) Cheon, C. H.; Joo, S.-H.; Kim, K.; Jin, J.-I.; Shin, H.-W.; Kim, Y.-R. *Macromolecules* **2005**, *38*, 6336.
- (14) Huang, B.; Li, J.; Jiang, Z.; Qin, J.; Yu, G.; Liu, Y. *Macromolecules* **2005**, *38*, 6915.
- (15) (a) Lee, J.-I.; Klarner, G.; Chen, J. P.; Scott, J. C.; Miller, R. D. *SPIE Int. Soc. Opt. Eng.* **1999**, *3623*, 2. (b) Hung, M.-C.; Liao, J.-L.; Chen, S.-A.; Chen, S.-H.; Su, A.-C. *J. Am. Chem. Soc.* **2005**, *127*, 14576.
- (16) Miteva, T.; Meisel, A.; Knoll, W.; Nothofer, H. G.; Scherf, U.; Müller, D. C.; Meerholz, K.; Yasuda, A.; Neher, D. *Adv. Mater.* **2001**, *13*, 565.
- (17) Jenekhe, S. A.; Osaheni, J. A. *Science* **1994**, *265*, 765.
- (18) Redecker, M.; Bradley, D. D. C.; Inbasekaran, M.; Woo, E. P. *Appl. Phys. Lett.* **1998**, *73*, 1565.
- (19) (a) Hou, Q.; Zhou, Q.; Zhang, Y.; Yang, W.; Yang, R.; Cao, Y. *Macromolecules* **2004**, *37*, 6299. (b) Kong, X.; Kulkarni, A. P.; Jenekhe, S. A. *Macromolecules* **2003**, *36*, 8992. (c) Wu, W.; Inbasekaran, M.; Hudack, M.; Welsh, D.; Yu, W.; Cheng, Y.; Wang, C.; Kram, S.; Tacey, M.; Bernius, M.; Fletcher, R.; Kiszka, K.; Munger, S.; O'Brien, J. *Microelectron. J.* **2004**, *35*, 343.
- (20) (a) Berggren, M.; Inganäs, O.; Gustafsson, G.; Rasmussen, J.; Andersson, M. R.; Hjertberg, T.; Wennerström, O. *Nature (London)* **1994**, *372*, 444. (b) Andersson, M. R.; Berggren, M.; Inganäs, O.; Gustafsson, G.; Gustafsson-Carberg, J. C.; Sele, D.; Hjertberg, T.; Wennerström, O. *Macromolecules* **1995**, *28*, 7525. (c) Buchgraber, C.; Pogantsch, A.; Kappaun, S.; Spanring, J.; Kern, W. *J. Polym. Sci., Part A: Polym. Chem.* **2006**, *44*, 4317. (d) Cong, Y.; Chen, Z.; Li, F.; Gong, Q. *Opt. Mater.* **2006**, *28*, 1084. (e) Chiang, C.-L.; Wu, M.-F.; Dai, D.-C.; Wen, Y.-S.; Wang, J.-K.; Chen, C.-T. *Adv. Funct. Mater.* **2005**, *15*, 231. (f) Lee, T.-W.; Park, O. O.; Cho, H. N.; Kim, Y. C. *Synth. Met.* **2002**, *131*, 129. (g) Lee, T.-W.; Ok Park, O.; Nam Cho, H.; Kim, Y. C. *Curr. Appl. Phys.* **2001**, *1*, 363.
- (21) (a) Chen, C. H.; Klubek, K. P.; Shi, J. U.S. Patent 5908581, 1999. (b) Chen, C. H.; Klubek, K. P.; Shi, J. U.S. Patent 5935720, 1999.
- (22) Coulson, D. R. *Inorg. Synth.* **1972**, *13*, 121.
- (23) Woods, L. L. *J. Am. Chem. Soc.* **1958**, *80*, 1440.
- (24) Liu, Y.; Liu, M. S.; Jen, A. K.-Y. *Acta Polym.* **1999**, *50*, 105.
- (25) Zhan, X.; Liu, Y.; Wu, X.; Wang, S.; Zhu, D. *Macromolecules* **2002**, *35*, 2529.
- (26) Wu, T.-Y.; Chen, Y. *J. Polym. Sci., Part A: Polym. Chem.* **2002**, *40*, 4570.
- (27) Peng, Q.; Lu, Z.-Y.; Huang, Y.; Xie, M.-G.; Han, S.-H.; Peng, J.-B.; Cao, Y.; Huang, W. *Macromolecules* **2004**, *37*, 260.
- (28) Ranger, M.; Rondeau, D.; Leclerc, M. *Macromolecules* **1997**, *30*, 7686.

- (29) Cho, H.-J.; Hwang, D.-H.; Lee, J.-I.; Jung, Y.-K.; Park, J.-H.; Lee, J.; Lee, S.-K.; Shim, H.-K. *Chem. Mater.* **2006**, *18*, 3780.
- (30) Miyaura, N.; Suzuki, A. *Chem. Rev.* **1995**, *95*, 2457.
- (31) Tokito, S.; Tanaka, H.; Noda, K.; Okada, A.; Taga, Y. *Appl. Phys. Lett.* **1997**, *70*, 1929.
- (32) (a) Chen, C. H.; Shi, J.; Tang, C. W. *Macromol. Symp.* **1997**, *125*, 1. (b) Jung, B.-J.; Yoon, C.-B.; Shim, H.-K.; Do, L.-M.; Zyung, T. *Adv. Funct. Mater.* **2001**, *11*, 430. (c) Kim, J. H.; Lee, H. *Chem. Mater.* **2002**, *14*, 2270.
- (33) Neher, D. *Macromol. Rapid Commun.* **2001**, *22*, 1365.
- (34) (a) Morgado, J.; Cacialli, F.; Friend, R. H.; Iqbal, R.; Yahioglu, G.; Milgrom, L. R.; Moratti, S. C.; Holmes, A. B. *Chem. Phys. Lett.* **2000**, *325*, 552. (b) Tang, C. W.; VanSlyke, S. A.; Chen, C. H. *J. Appl. Phys.* **1989**, *65*, 3610.
- (35) Kulkarni, A. P.; Zhu, Y.; Jenekhe, S. A. *Macromolecules* **2005**, *38*, 1553.
- (36) Ding, L.; Bo, Z.; Chu, Q.; Li, J.; Dai, L.; Pang, Y.; Karasz, F. E.; Durstock, M. F. *Macromol. Chem. Phys.* **2006**, *207*, 870.

MA071271Y